

## Formation of CrSi and CrSi<sub>2</sub> upon annealing of Cr overlayers on Si(111)

P. Wetzel, C. Pirri, J. C. Peruchetti, D. Bolmont, and G. Gewinner

*Laboratoire de Physique et de Spectroscopie Electronique, Faculté des Sciences et Techniques,  
Université de Haute Alsace, 4, rue des Frères Lumière, 68093 Mulhouse Cedex, France*

(Received 10 November 1986)

The evolution of the Cr/Si(111) interface upon thermal processing is investigated by low-energy electron diffraction (LEED), angle-resolved ultraviolet, and x-ray photoemission spectroscopy. Increasing progressively the annealing temperature and time results in the successive formation of CrSi and CrSi<sub>2</sub>, two well-defined bulk silicides. The silicides are characterized by their valence-band and core-level spectra. It is found that in contrast to CrSi<sub>2</sub>, CrSi exhibits a high density of states at the Fermi energy, which is reflected in the core-level spectra. As to the silicide film structure, the LEED data indicate that for large Cr-layer thicknesses [ $\geq 80$  monolayers (ML)] the silicides are apparently polycrystalline but, at lower coverages ( $\leq 30$  ML), epitaxial domains for both CrSi and CrSi<sub>2</sub> can be achieved.

Investigation of the silicon-transition-metal interfaces has been considerably expanded in recent years. Clearly both technological interests and fundamental reasons explain the motivation for such studies. The possibility of stable, definite, eventually epitaxial silicide film formation on Si surfaces has a great number of potential applications in microelectronics. Among such systems Cr/Si(111) seems to be of special interest since there is an excellent lattice match of the hexagonal structure of the CrSi<sub>2</sub> (0001) plane and Si(111). Epitaxial growth of CrSi<sub>2</sub> on Si(111) was therefore expected and actually observed.<sup>1,2</sup> Yet until now little work has been devoted to the study of Cr silicide formation on Si(111) using surface techniques. Photoemission studies of the interface formed at room temperature have demonstrated that Cr reacts very strongly with Si but the intermixed overlayer obtained in this way cannot be identified as one of the known bulk silicides.<sup>3,4</sup> However annealing resulted in the formation of CrSi<sub>2</sub> and it is usually believed that only the latter silicide can be prepared by thermal processing of a Cr overlayer condensed on Si(111) at room temperature.<sup>5</sup> In this report we present the results of an annealing study of Cr overlayers on Si(111), concentrating more specifically on thick overlayers [ $\geq 80$  monolayers (ML)]. We present evidence that while CrSi<sub>2</sub> is formed by prolonged annealing at higher temperatures ( $\sim 450^\circ\text{C}$ ), milder annealing results in the formation of CrSi. Both compounds can be readily distinguished by their respective valence and core-level photoemission signatures. For the sake of completeness we also mention some interesting results concerning thinner Cr overlayers ( $\leq 30$  ML), in particular the possibility of epitaxial growth of both CrSi and CrSi<sub>2</sub>.

All experiments were carried out *in situ* in a ultrahigh-vacuum (UHV) chamber (base pressure  $\sim 5 \times 10^{-11}$  Torr) equipped for low-energy electron diffraction (LEED) and angle-resolved ultraviolet (ARUPS) and x-ray (XPS) photoemission measurements. Absolute values for the work function  $\phi$  were evaluated by measuring the width of the photoemission energy distribution curves at normal emission with the sample biased by a negative voltage of

$-10.00$  V with respect to the ground. The typical angular and energy resolution are  $\sim 3^\circ$  and  $\sim 0.2$  eV, respectively. After standard surface cleaning of the *n*-type Si(111) substrate (resistivity about  $1 \Omega \text{ cm}$ ) by ion bombardment and thermal annealing cycles, chromium layers of various thicknesses were condensed onto the surface from a home made Cr source operating typically at a pressure of  $5 \times 10^{-10}$  Torr and a rate of 3 Å/min. The interface formed at room temperature (RT) was subsequently stepwise heated under UHV in the temperature range  $200\text{--}600^\circ\text{C}$  for durations up to 15 min. The temperature was evaluated by means of a thermocouple, spot welded onto the Ta sheet supporting the sample. All spectra presented here are recorded with He<sub>I</sub> (21.22 eV) and Mg K $\alpha$  (1253.6 eV, unmonochromatized) photon excitation.

First we present the annealing experiments performed on an 80-ML Cr layer condensed on Si(111) at room temperature. These data are typical for thick Cr films ( $\Theta \geq 80$  ML). Our measurements on interfaces formed at RT (Ref. 6) indicate that at lower Cr thicknesses ( $\sim 30\text{--}40$  ML) the surface layer ( $\sim 5$  Å) of the condensed film still differs significantly from pure Cr metal in agreement with previous work.<sup>3</sup> Even at RT there is considerable Cr-Si intermixing. The results are summarized in Figs. 1–4. Figure 1 shows the valence-band spectra at normal emission reflecting the electronic structure of the probed top layer ( $\sim 5$  Å for UPS) as a function of annealing. In Fig. 2 we display the relevant changes in the ratio of the XPS Cr  $2p_{3/2}$  and Si  $2p$  core-level intensities for two polar emission angles:  $\theta = 45^\circ$  and  $70^\circ$ , i.e., respectively bulk- and surface-sensitive geometries. Finally, Figs. 3 and 4 present the data on XPS core line shifts, widths, and asymmetries as well as work-function measurements. The typical annealing steps discussed below are indicated in the figures.

After Cr evaporation onto the Si(111) surface kept within  $50^\circ\text{C}$  of RT the probed overlayer seems to be a fairly uniform Cr-metal film in contrast with the result of a similar study of the Co/Si(111) system.<sup>7</sup> This is inferred from XPS measurements at  $\theta = 70^\circ$  which indicate

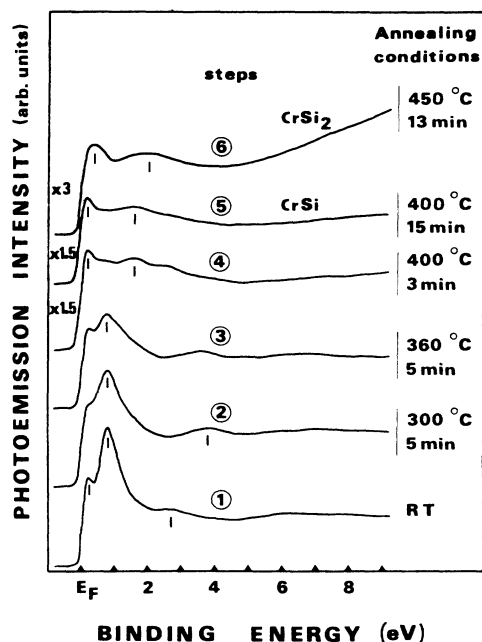


FIG. 1. Normal emission ARUPS curves from a 80-ML Cr deposit on Si(111) as a function of annealing. Definite silicide formation as well as the various annealing steps are indicated.

that the Si  $2p$  line is undetectable at 80 ML Cr coverage. Only incoherent scattering is observed by LEED and the ARUPS spectrum (step 1 in Fig. 1) is typical for pure polycrystalline Cr metal with peaks at  $\sim 0.2$ ,  $0.8$ , and  $2.8$  eV binding energy. The peak at  $0.8$  eV shows an important oxygen contamination sensitivity suggesting that it is, at least in part, connected with the surface electronic structure. Both the work-function and core-level data also agree with measurements on bulk polycrystalline Cr samples.

Annealing at  $300^\circ\text{C}$  for 5 min (step 2) results in the appearance of Si atoms in the probed region. It can be seen from Fig. 3(a) that the Si  $2p$  binding energy is  $\sim 99.0$  eV

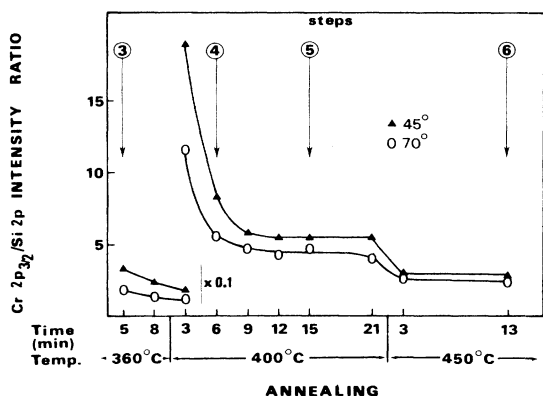


FIG. 2. Evolution of the Cr  $2p_{3/2}$  to Si  $2p$  core-level intensity ratio upon annealing 80 ML of Cr on Si(111). The polar emission angle corresponds either to bulk ( $45^\circ$ ) or to surface ( $70^\circ$ ) sensitivity.

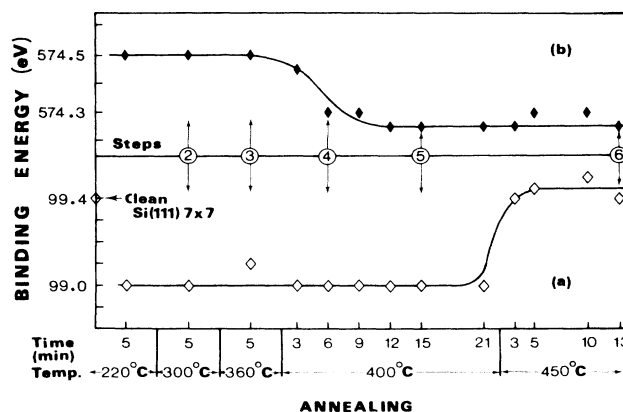


FIG. 3. Change in the core-level binding energy on annealing 80 ML of Cr on Si(111): (a) Si  $2p$ ; (b) Cr  $2p_{3/2}$ .

rather than  $\sim 99.4$  eV for monocrystalline Si. Exactly the same core line shift was observed in our previous annealing study of an oxidized Cr overlayer on Si(111).<sup>8</sup> This is characteristic of Si in a metal-rich environment and may be the result of enhanced final-state relaxation for Si atoms embedded in a metal. Considering now the relevant ARUPS curve in Fig. 1 we observe a strong attenuation of the  $0.8$ -eV feature and the appearance of a shoulder at  $\sim 3.8$  eV. Photoemission data of Si chemisorbed on transition metals such as Fe (Ref. 9) suggest that the latter peak should reflect Si  $3p$  valence-band emission from Si species either segregated at the Cr surface or present in the Cr film in a dilute state as a result of diffusion. The rapid attenuation of the  $0.8$ -eV peak probably results from modifications in the bulk and/or surface electronic structure of Cr induced by the presence of Si species.

Upon further annealing at  $360^\circ\text{C}$  for 5 min (step 3) we essentially observe that the trend apparent at step 2 is

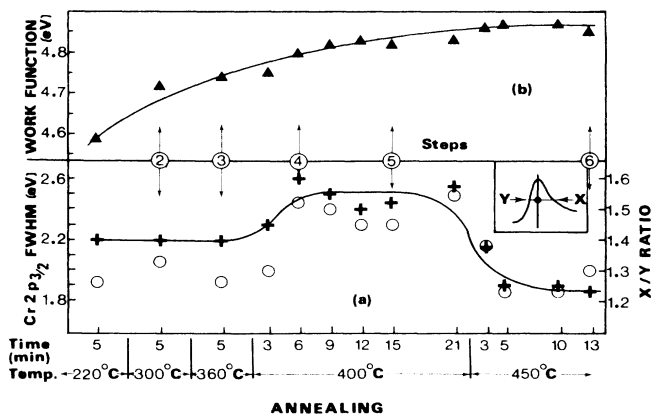


FIG. 4. Evolution observed on annealing an 80-ML Cr deposit on Si(111): (a) +, full width at half maximum (FWHM) of the Cr  $2p_{3/2}$  core line.  $\circ$ , asymmetry parameter of the Cr  $2p_{3/2}$  core line defined as the ratio  $X/Y$  of the half widths at half maximum measured on the high- and low-binding-energy sides of the core line, respectively (see insert). (b) Work function.

strongly reinforced. The drastic reduction of the 0.8-eV peak in the ARUPS spectrum as well as the decrease in the Cr  $2p_{3/2}$  to Si  $2p$  intensity ratio clearly demonstrate the diffusion of Si species through the Cr film. Simultaneously the work function increases progressively. At this stage, however, the overlayer still exhibits, as far as XPS and UPS spectra are concerned, the essential properties of bcc Cr metal, albeit "contaminated" by Si.

Increasing the annealing temperature up to 400°C (step 4) results in important changes indicating a qualitative modification of the overlayer. This can best be seen in the ARUPS data. While the 0.8-eV peak is still visible, new features appear at 0.2 and 1.6 eV, suggesting the presence of a new surface compound. Also a small shift as well as a broadening and skewing of the Cr  $2p_{3/2}$  core line can now be detected (Figs. 3 and 4). Clearly these observations can be traced back to changes in the chemical nature of the film.

Further increasing the annealing time at 400°C up to 15 min (step 5) induces both XPS and UPS evolution which confirm the formation of a definite silicide. Considering the data of Fig. 2 it is apparent that at this stage the Cr  $2p_{3/2}$  to Si  $2p$  intensity ratio shows a well defined plateau. The relevant stoichiometry is CrSi since the core-level intensity ratio is actually close to twice the value measured on CrSi<sub>2</sub> crystals. Thus at this stage we believe that well-defined CrSi has been formed. The compound seems to be either polycrystalline or amorphous since LEED shows diffuse scattering. The plateau in the XPS intensity data is also reflected in the Cr  $2p_{3/2}$  line position, shape and width. The chemical shift observed between Cr metal and CrSi is ~0.25 eV. The change in the Cr  $2p_{3/2}$  core line shape in passing from Cr metal to CrSi deserves some comments. As can be seen from the data in Fig. 4(a) the line becomes quite asymmetric and significantly broadened. This behavior may be explained by an inhomogeneous nature of the overlayer film, i.e., the presence of two (or more) unresolved chemically shifted components. However since the stoichiometry and UPS data strongly suggest the presence of a definite compound it is expected that the Cr  $2p$  core-level spectrum exhibits one unique characteristic line rather than two components. Thus, while one cannot rule out the presence of chemically shifted components, we rather suggest an alternative explanation in terms of Fermi-surface excitation effects on the x-ray photoemission line shape.<sup>10</sup> In particular the strong asymmetry can be interpreted as originating from satellite excitation. Photoemission is a many-electron process in which the photoionization of a core level may be accompanied by an excitation of a filled-valence-state electron just below into an empty state just above the Fermi energy  $E_F$ . Since there is a continuous distribution of states in metals a tail develops on the high-binding-energy side of the core line. Roughly, a higher density of states near  $E_F$  results in a more important tail and in turn in an enhanced broadening and asymmetry of the core line. These considerations imply that the density of states at  $E_F$  is higher in CrSi than in bcc Cr metal. In this respect, it is well known that in bcc Cr metal the Fermi level is located near a minimum in the density of states between bonding and antibonding  $d$  states.<sup>11</sup> In contrast, calcula-

tions for CrSi (Ref. 4) predict a peak in the density of states close to  $E_F$ . These states show nonbonding character and are localized on the Cr species. Thus, it is expected that because of the localized nature of photoionization, only Cr core lines are affected by satellite excitation. The Si  $2p$  line shape should not be modified in agreement with experiment. It can be seen in Fig. 1 that photoemission confirms the presence of a high density of states at  $E_F$  in CrSi since we observe a prominent peak at 0.2 eV in the CrSi spectrum. This feature reflects emission from nonbonding Cr  $d$  states while the peak at ~1.6 eV can be attributed to bonding states derived from Cr  $3d$ -Si  $3p$ . The agreement of the experimental spectrum with the calculated density of states is fairly good.<sup>4</sup> Yet, as in the case of CrSi<sub>2</sub>, bonding states are predicted at somewhat higher binding energies (0.5-1 eV) than observed experimentally. This might be the result of correlation effects which are important in the case of transition metal compounds and usually difficult to take into account theoretically. Note also that both experiment and calculations agree in the trend observed for the bonding states energy location in passing from CrSi<sub>2</sub> to CrSi, i.e., a shift toward the Fermi energy of ~0.5 eV.

Drastic changes in the spectroscopic data are brought about by further heating at 450°C for 13 min (step 6). Again at this stage the Cr  $2p_{3/2}$  to Si  $2p$  intensity ratio in Fig. 2 displays a plateau, corresponding to a stoichiometry of CrSi<sub>2</sub>. The core-level position, shape, and width as well as the work function also exhibit a plateau and both XPS and ARUPS data are now typical for chromium disilicide.<sup>3,4,8</sup> The Si  $2p$  binding energy is raised by ~0.5 eV, the work function is near 4.85 eV and the Cr  $2p_{3/2}$  line-shape asymmetry is strongly reduced with respect to CrSi. Again let us comment on the latter effect. According to the discussion presented above this finding implies a drastic drop in the density of states at  $E_F$ . Indeed it is apparent in Fig. 1 that the ARUPS data support this interpretation. CrSi<sub>2</sub> exhibits a much lower density of states at  $E_F$  than CrSi in agreement with the calculations by Bisi and Calandra.<sup>4</sup> Actually CrSi<sub>2</sub> has been reported to be a metal by some authors and a small-gap semiconductor by others.<sup>12,13</sup> Finally, at this step, it is noteworthy that LEED does not show any pattern characteristic of epitaxial CrSi<sub>2</sub>.

Concluding this discussion we notice that throughout the experiment (except the very beginning steps 1,2) the Cr  $2p_{3/2}$  to Si  $2p$  core line intensity ratio is always lower at  $\theta=70^\circ$  than  $\theta=45^\circ$  indicating some surface segregation of Si in particular on CrSi and CrSi<sub>2</sub>.

In summary we have shown that on annealing an 80-ML Cr film on Si(111), the definite CrSi silicide is formed as an intermediate step ruling out that only the CrSi<sub>2</sub> disilicide end product can be formed in this way as usually believed. In this respect one may wonder whether or not the same behavior would be observed starting with thin Cr films ( $\leq 30$  ML) where strong intermixing occurs already at RT. Preliminary measurements suggest that for coverages above ~3 ML, CrSi silicide formation first occurs upon mild annealing before any nucleation of CrSi<sub>2</sub>. The disilicide appears as a further step in the annealing process. The evidence which comes again from

XPS and ARUPS but also from LEED observations will be reported in more detail elsewhere.<sup>14</sup> Let us just mention here that in agreement with previous work<sup>1,15</sup> various ordered LEED patterns can be observed upon annealing thin Cr films. In particular a  $\sqrt{3}\times\sqrt{3}R30^\circ$  pattern is observed as an intermediate step in the formation of the  $1.17\times 1.17$  patterns typical for epitaxial  $\text{CrSi}_2$ . We suggest that the  $\sqrt{3}\times\sqrt{3}$  diagram originates from epitaxial  $\text{CrSi}$  whose crystallographic structure is cubic ( $B20$ ,  $\text{FeSi}$  type). The lattice mismatch for the epitaxial relationship  $\text{CrSi}(111)/\text{Si}(111)$  is only 1.6%. The  $\text{CrSi}(111)$  lattice plane corresponds to the  $\sqrt{3}\times\sqrt{3}$  sublattice of  $\text{Si}(111)$ . As to the  $\text{CrSi}_2$  epitaxy, we always observed the presence of two kinds of  $\text{CrSi}_2$  domains corresponding to

$1.17\times 1.17R30^\circ$  and  $1.17\times 1.17R0^\circ$  LEED reflections respectively. Generally we found that the microstructure of the  $\text{Cr}/\text{Si}(111)$  appears to be quite complicated depending on such usual parameters as overlayer thickness and annealing but also on finer details in the preparation procedure. This is in agreement with the rather complex behavior revealed in recent work on  $\text{Co-Si}(111)$  (Ref. 16) and  $\text{Ti}/\text{Si}(111)$  (Ref. 17) by Chambers and co-workers.

#### ACKNOWLEDGMENT

This work was supported by the Centre National d'Etudes des Télécommunications under Contract No. 85 3B 070 CNS.

<sup>1</sup>K. Oura, S. Okada, and T. Hanawa, in Proceedings of the 8th International Vacuum Congress, Cannes (France), 1980, edited by F. Abeles and M. Croset [Suppl Revue Le Vide, Les Couches Minces **201**, 181 (1981)].

<sup>2</sup>F. Y. Shiau, H. C. Cheng, and L. J. Chen, Appl. Phys. Lett. **45**, 524 (1984).

<sup>3</sup>A. Franciosi, D. J. Peterman, J. H. Weaver, and V. L. Moruzzi, Phys. Rev. B **25**, 4981 (1982).

<sup>4</sup>A. Franciosi, J. H. Weaver, D. G. O'Neill, F. A. Schmidt, O. Bisi, and C. Calandra, Phys. Rev. B **28**, 7000 (1983).

<sup>5</sup>K. N. Tu, in *Thin Film, Interdiffusion and Reactions*, edited by J. M. Poate, K. N. Tu, and J. W. Mayer (Wiley, Chichester, England, 1978).

<sup>6</sup>P. Wetzel *et al.* (unpublished).

<sup>7</sup>C. Pirri, J. C. Peruchetti, G. Gewinner, and D. Bolmont, Solid State Commun. **57**, 361 (1986).

<sup>8</sup>P. Wetzel, C. Pirri, J. C. Peruchetti, D. Bolmont, and G. Gewinner, Surf Sci. **178**, 27 (1986).

<sup>9</sup>B. Egert, H. J. Grabke, Y. Sakisaka, and T. N. Rhodin, Surf Sci. **141**, 397 (1984).

<sup>10</sup>G. K. Wertheim and P. H. Citrin, in *Photoemission in Solids I*, edited by M. Cardona and L. Ley (Springer, Berlin, 1978).

<sup>11</sup>M. Asdente and J. Friedel, Phys. Rev. **124**, 384, (1961).

<sup>12</sup>J. P. Suchet, in *Crystal Chemistry and Semiconduction in Transition Metal Binary Compounds* (Academic, New York, 1971).

<sup>13</sup>F. Nava, T. Tien, and K. N. Tu, J. Appl. Phys. **57**, 2018 (1985).

<sup>14</sup>P. Wetzel *et al.* (unpublished).

<sup>15</sup>V. G. Lifshits, V. G. Zavodinskii, and N. I. Plyusnin, Phys. Chem. Mech. Surfaces **2**(3), 784 (1984).

<sup>16</sup>S. A. Chambers, S. B. Anderson, H. W. Chen, and J. H. Weaver, Phys. Rev. B **34**, 913 (1986).

<sup>17</sup>S. A. Chambers, D. M. Hill, F. Xu, and J. H. Weaver, Phys. Rev. B **35**, 634 (1987).